Investigating the Performance of a Semi-Professional Magnetometer for Space Weather Research: 13 Years of Measurements from a Backyard in Anchorage

William H. Barndt, Doğacan S. Öztürk, Whitham Reeve

University of Alaska Fairbanks, Geophysical Institute, Space Weather UnderGround (SWUG)
whbarndt@alaska.edu, dsozturk@alaska.edu

May 23rd, 2023

Space weather is an important field of study for Alaska as it can impact the everyday lives of Alaskans. One way that Space Weather can cause disruptions is through geomagnetically induced currents (GICs) which can occur along power transmission lines, pipelines, and railroads. Geomagnetic disturbance measurements are one way of studying when and where GICs can occur which is essential for safeguarding Alaska's infrastructure. The Space Weather UnderGround (SWUG) project, founded by Charles Smith at the University of New Hampshire, was created to increase measurements of geomagnetic disturbances by deploying low-cost arrays of magnetometers using Simple Aurora Monitors (SAMs) provided by Whitham Reeve. In 2020, the University of Alaska Fairbanks developed their own SWUG program for understanding these geomagnetic disturbance effects in Alaska. This project's research was motivated by investigating the capabilities of SAM-III, for understanding Space Weather related disturbances. I obtained a unique dataset of SAMIII data, curated by Whitham Reeve, spanning at least one solar cycle, and developed tools and datasets to analyze and study it by first comparing it to Narod science-grade magnetometers deployed across Alaska as a part of the Geophysical Institute Magnetometer Array (GIMA). I (Barndt) investigated the dependencies of this semi-professional magnetometer scientifically and operationally by analyzing its relation to the solar cycle and subsurface temperature at Eagle River close to where it is deployed. With these analyses, I was able to evaluate the performance of SAM-III and provide guidance for optimizing its performance for GIC research.

Introduction

Whitham Reeve curated over 13 years of Simple Aurora Monitor (SAM) magnetometer data from 2009 to present – 2 years of a 1-axis SAM, from 2009 to 2010, and 12 years of a 3-axis SAM (called SAM-III) data, from 2010 to 2022. The focus of this project was to conduct a preliminary investigation into the scientific and operational dependencies of SAM-III given this large-spanning dataset. The first goal was to compare the data provided with a science-grade magnetometer nearby for a qualitative and quantitative comparison. This was chosen to be a Narod magnetometer in Trapper Creek, a part of the Geophysical Institute Magnetometer Array (GIMA). Given that the SAM-III data encompasses a whole solar cycle, we would then look at solar sunspot information investigate its scientific dependencies since the number of sunspots correlates with which stage of the solar cycle the sun is located, the two major stages being the solar maximum or the solar minimum. Lastly, understanding that SAM-III magnetometers have temperature dependencies, we would look at the subsurface temperature nearby to see its impact operationally.

Geomagnetic Disturbances

Geomagnetic disturbances in Earth's magnetosphere can occur due to interactions with the solar wind and space weather events and can generate Geomagnetically Induced Currents (GICs). These GICs can cause significant impact to long ground-based conductive infrastructure such as damage to high-voltage power transmission systems or railway systems and increased corrosion of gas and oil pipelines. [1] One way of measuring these geomagnetic disturbances is using a magnetometer. As a reminder, geomagnetically induced currents are governed by Faraday's Law of Induction, equation (1), in electrodynamics which states that a change in the magnetic field with time can cause a change in the electric field in space, which can constitute a current.

$$\nabla \times \mathbf{E} = -\partial \mathbf{B}/\partial t \tag{1}$$

Space Weather UnderGround (SWUG) Program

The Space Weather UnderGround (SWUG) Program, founded by Dr. Charles Smith at the University of New Hampshire, is an educational outreach program geared towards undergraduate and high school students to build and deploy a cost-effective and research-capable array of magnetometers across Alaska. The magnetometers used by SWUG are called Simple Aurora Monitors (SAMs).

3-Axis Simple Aurora Monitor (SAM-III)

3-Axis Simple Aurora Monitor (SAM-III) is a semi-professional magnetometer designed by Dirk Langenbach and Karsten Hansky and developed by Reeve Engineers, founded by Whitham Reeve, who distributes SAM-III kits to both the University of Alaska Fairbanks and the University of New Hampshire SWUG programs. [2] SAM-III is a magnetometer kit that consists of a main controller printed circuit board (PCB), keyboard PCB, a Liquid Crystal Display (LCD) module, three fluxgate magnetometer sensors and includes an option for a temperature sensor. Generally, magnetometers have a dependency on temperature and it varies with magnetometer setups. The SAM-III fluxgate magnetometer sensor is very sensitive to temperature variations. The temperature coefficient is approximately −100 to −150 nT/°C (the minus sign indicates that the amplitude increases as the temperature decreases). (pg. 66) [3] SAM-III's sensor has a range of approximately ±50,000 nT with a resolution of 1 − 2 nT. (pg. 2) [3] The data typically has a temporal resolution of 1 second however the data provided by Whitham Reeve had a temporal resolution of 10 seconds.

Methodology

The SAM-III dataset provided by Whitham Reeve included .log, .sam, .png, and .txt files for each day for the years 2010 through 2022. The .log files include information on the number of correct and erroneous lines of readings for that day and what the erroneous lines were read as. The .sam files give metadata on the components, date, location, author and what each reading is for each component subtracted by a baseline. The .png files show a time series plot of baseline subtracted data for each component for that day, these are created from the .sam files. Lastly, the .txt files include the raw magnetometer data for each reading and each component. [4] These .txt files are the files that were parsed through to use for this project. This data included the 'datetime' of the reading and x, y, and z components of the magnetic field.

The tools used for parsing and analyzing the data were the Python programming language with the Pandas data analysis library [5]. Using these tools, I created a toolset of scripts to work with this data. In Figure 1 you can see the Architecture Diagram of the scripts created during the duration of the project.

The SAM-III dataset included various files on measurement information but the .txt files for each day were used to extract the magnetometer data. In the diagram, I represented these .txt files as the RAW SAIII .txt files and created the SAM-III_data_parser.py script to process the files into a Python readable format. After parsing the .txt files, the non-erroneous data was read into a pandas DataFrame with the rows representing each measurement and columns representing the date, time and magnetic field component information for each measurement. It was then exported to a .pickle file, a serialized representation of the Pandas DataFrame object, used for ease of transfer and internal Python readability, so the raw data can be manipulated and, if needed, reviewed with ease. Afterwards, the raw SAM-III data .pickle files are then processed to a standard data format, used so that both magnetometer's data can be analyzed on a similar footing. This format first baseline subtracts all of the readings, where, for each day, each reading is subtracted by the first reading of that day. This allows normalization of the values to directly see the changes for that day and to be able to compare it to measurements from other instruments easier. Then, a new coordinates system, made of *H*, *D*, and *Z* components, is calculated from the *x*, *y*, and *z* coordinate measurements. Figure 2 is a visualization of this coordinate system. The *Z*-component is the same as in the *x*, *y*, *z* system however *x* and *y* transformed using equations (2) and (3).

$$H = \sqrt{X^2 + Y^2} \tag{2}$$

$$D = \tan^{-1}\left(\frac{y}{x}\right) \tag{3}$$

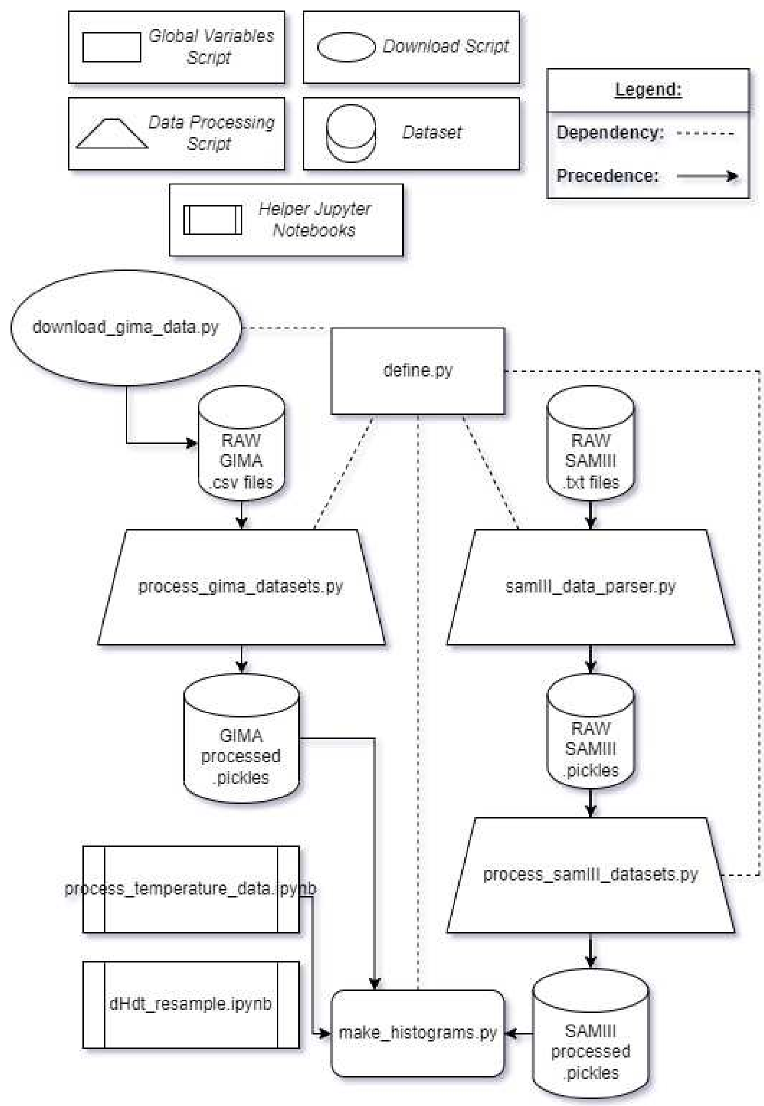

Figure 1: Architecture Diagram of the scripts used during the project. [6]

This coordinate system is useful because geomagnetic activity and disturbances occur more often in the horizontal component than the *z*-component which allows us to couple the *x* and *y* measurements into one value. With this *H*-component, δH, the difference in the current *H* and the previous, is calculated and δt, the difference in time, is calculated to then calculate $\partial H/\partial t$, the change in the H-component in time for each reading.

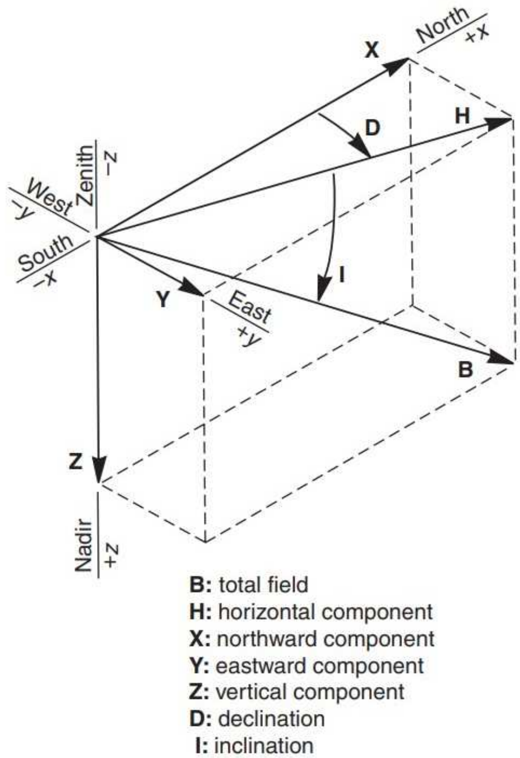

Figure 2: H, D, Z Coordinate System. [7]

Geophysical Institute Magnetometer Array (GIMA)

The Geophysical Institute Magnetometer Array (GIMA) is comprised of thirteen science-grade magnetometer stations dispersed across Alaska. Each station includes a Narod ring-core, fluxgate magnetometer [8], GPS clock and data logger which then transfers the data collected to the Geophysical Institute for verification, to archive and make available to the broader space weather science community. [9] This data can be retrieved publicly from the GI's website [10] and it can be shown graphed as the H, D, Z components with the median of the day subtracted from the readings. As of May 23rd, 2023, the H, D, Z components of GIMA physically correspond to x, y, and z components respectively. The temporal resolution of the readings for GIMA magnetometers is 1 second.

The GIMA magnetometer used was from GIMA's Trapper Creek site about 75 miles north of Anchorage (roughly 0.97 degrees geographic latitude and 0.27 degrees geographic longitude) and is roughly similar in magnetic latitude and longitude. This GIMA site was chosen due to its close distance to Anchorage but also due to its overlap in the time the data was taken — it covered all the years of Reeve's SAM-III data from 2010 to 2023. This data was retrieved from GIMA Magnetometer Archive of the Geophysical Institute [11]. The data was downloaded in a .csv file format for each day which contained information on the datetime of the reading and x, y, and z components of the magnetic field. The process of subtracting the start of the day from the daily readings and the coordinate and differential calculations are done the same as the GIMA dataset, converting the GIMA dataset into the same standard format talked about earlier.

Scientific and Operational Analyses Datasets

The two other datasets used in the final analysis were the yearly mean total sunspot number and the yearly mean subsurface temperature. The yearly mean total sunspot number dataset was retrieved from the Sunspot Index and Long-term Solar Observations website [12] in a .csv file which covers the years 1700 to the present. The subsurface temperature data was retrieved by the Alaska Road Weather Information System on the Iowa State University website. [13] Multiple stations' subsurface temperature data was retrieved that was nearby either Trapper Creek's GIMA magnetometer or Reeve's SAMIII magnetometer in Anchorage. This data was downloaded as .xlsx files which were then converted to .csv files to be read into Python. Station GWSA2 in Eagle River was selected for the subsurface temperature comparison due to the largest continuous data that overlapped with the years of the magnetometer data. This data covered years 2011 through 2019 with hourly readings which were then averaged together and exported as a .pickle file in the process_temperature_data.ipynb notebook to form the yearly mean subsurface temperature. After each of these datasets was created and processed, they were then read into the make_histograms.py script to start the analysis.

Results

The goal of this project was to analyze the SAM-III dataset scientifically and operationally. This was done by comparing each year and how many days in that year there were readings above a certain threshold and comparing it to sunspot and subsurface temperature data. Figure 3, 4, 5, and 6 show how well SAM-III read *H*-component events over a certain threshold of the strength of the magnetic field compared with the Trapper Creek GIMA magnetometer. Figure 7 shows this for the *z*-component for over a threshold of 100 nT.

These figures were created from the SAM-III and GIMA standard format datasets, where both included datetime *x, y, z, H, D, δH, δt, δH/δt*, information for each reading. Both datasets were first resampled into minute readings for ease of processing time during figure creation since standard format SAM-III data constituted roughly 2 GB of data and standard format GIMA data was roughly 20 GB. Afterwards, these resampled datasets were used in the make_histograms.py script to create the histograms in these figures. This was done by first filtering out the data not within the thresholds then resampling again, instead to daily readings. [6]

H- and *Z*-Component Threshold Analyses

In these plots, you can see the comparison between SAM-III and GIMA and their number of days with readings above 250 nT and 500 nT for each year with the year values for sunspot number and subsurface temperature. The first thing to note is how well SAMIII and GIMA's counts for each component are comparable to each other. Most years have roughly similar counts with GIMA typically having more than SAM-III. The next is readings from SAM-III and GIMA generally show a solar cycle dependence with the solar maximum, the period of greatest solar activity, being around 2015-2016 and the solar minimum, the period of the lowest solar activity, around 2019-2020.

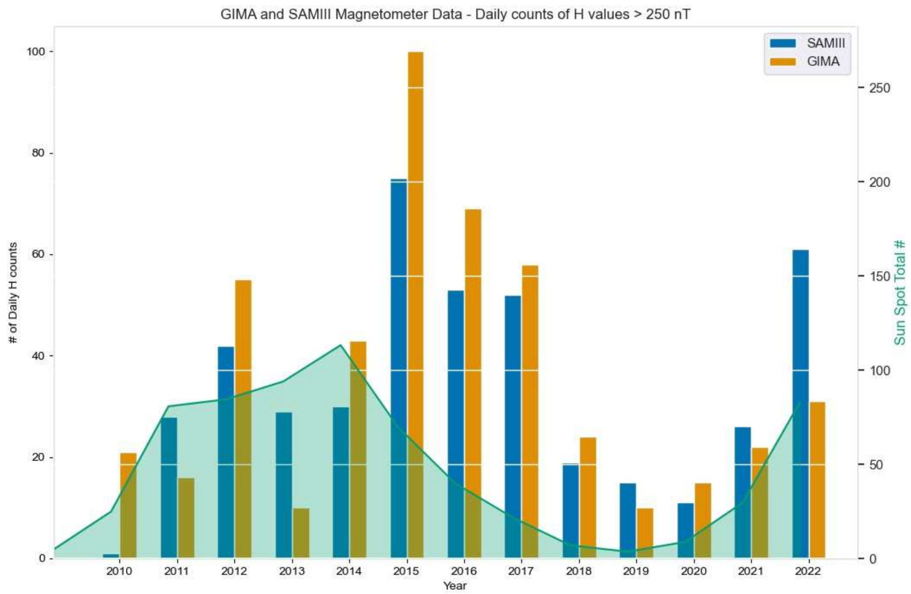

Figure 3: Number of days with |H| > 250 nT compared with the sunspot number

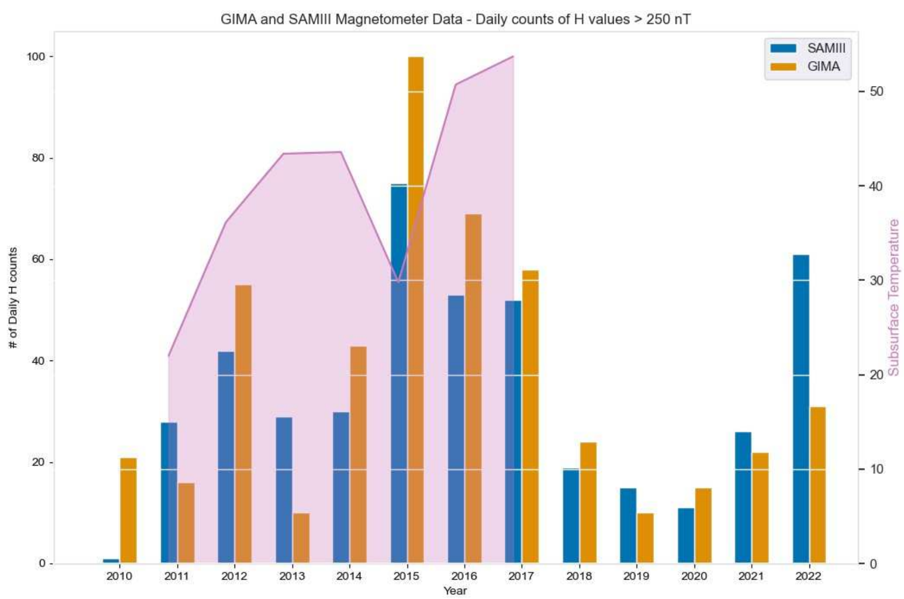

Figure 4: Number of days with |H| > 250 nT compared with the subsurface temperature

The peak of that solar cycle was in 2014 when the yearly mean sunspot count is the greatest. However, the counts for both SAM-III and GIMA are at their peak the following year. This is generally seen to be the case and has been shown in other observations [14]. Thus, it seems both SAM-III and GIMA are reliable in providing information on solar activity and space weather events. For the operational analysis, there didn't seem to be any direct correlation between the number of days above the threshold and the yearly mean subsurface temperature from Eagle River and a more granule look at the temperature data is necessary to better see temperature variation with the SAM-III magnetometer.

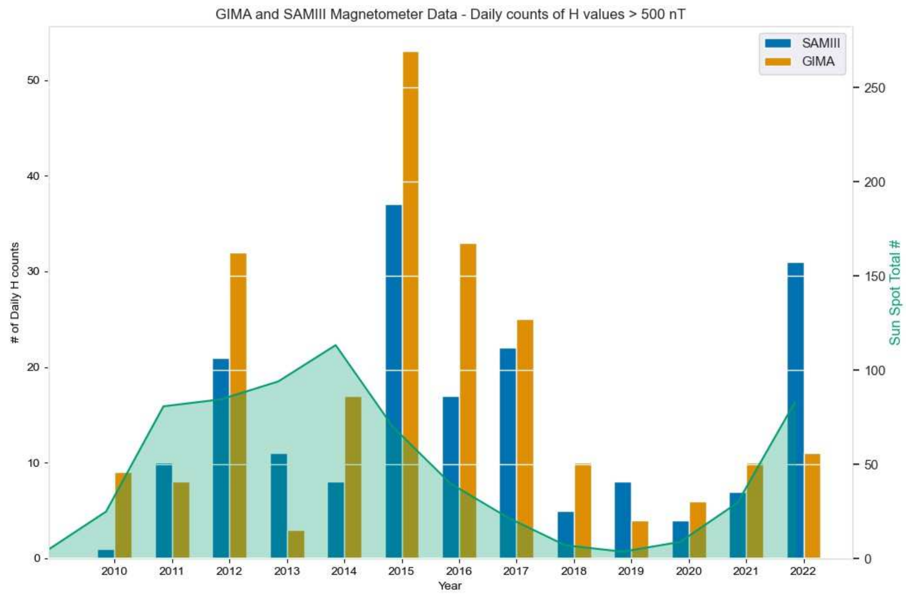

Figure 5: Number of days with |H| > 500 nT compared with the sunspot number

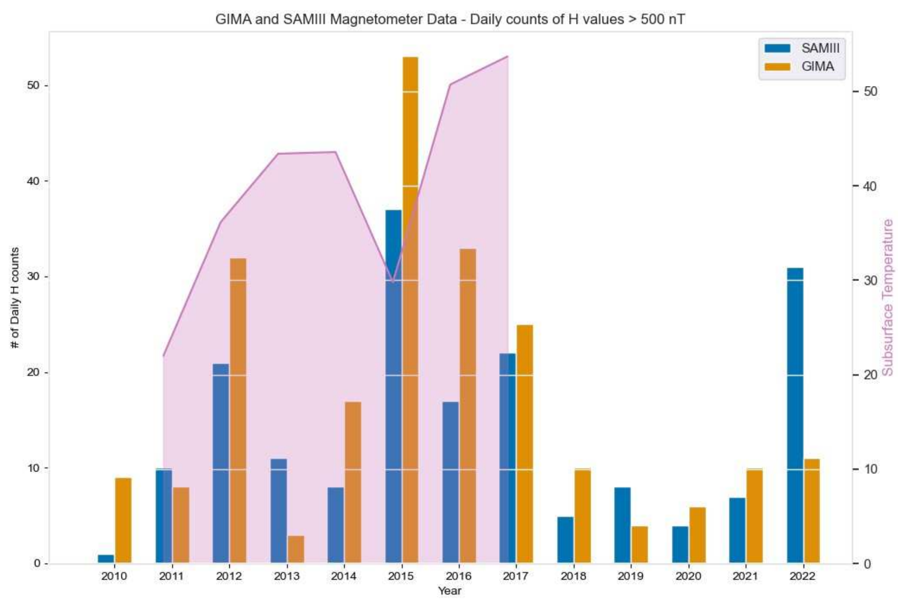

Figure 6: Number of days with |H| > 500 nT compared with the subsurface temperature

$\delta H/\delta t$ Threshold Analyses

The next analysis was looking at the change in the magnetic field in time, or $\delta B/\delta t$. Purely looking at the horizontal component H, we looked at two thresholds, 6 nT/s and 20 nT/s, shown in figures 8 and 9. These thresholds were chosen based on other research that has been done with measuring geomagnetic disturbances. [15]

These sets of plots don't include the subsurface temperature comparison since when $\delta H/\delta t$ is calculated the baseline dependence of temperature is mostly eliminated in the first order. It's important to note that these plots are in log scale and it can be seen that GIMA's magnetometer readings for both thresholds are roughly an order of magnitude larger than SAM-III readings. This seems to be an issue with the temporal resolutions of both datasets. GIMA's magnetometer data had a temporal resolution of 1 second and this implementation of the SAM-III device had a temporal resolution of 10 seconds. One analysis that could be done to further look into this would be to resample the GIMA dataset into 10-second readings first then calculate $\delta H/\delta t.$ instead of the inverse, then compare the results of each $\delta H/\delta t$.

Anomalies and Erroneous Data

Anomalies

There were two notable anomalies found in this analysis, the first being some of the SAMIII data in the year 2022. In Figure 10 and 11 you can see two anomalous phenomena: a steady increase in magnetometer readings from 6:00 UTC to roughly 16:00 UTC and a discontinuity at 18:00 UTC. The first anomaly is hypothesized to be due to temperature variability with the magnetometer sensor, however further investigation into SAM-III's temperature dependencies is needed before a conclusion can be made. This is actively underway with future SAM-III devices which include a temperature sensor. The second anomaly is unknown but it seems like it could be that the baseline subtraction calculation made for these plots stopped at 18:00 UTC and so the figure plots the absolute magnetic field. There might be more anomalies in the 2022 data and other years but these were the first major found near the end of this project.

The latter anomaly doesn't seem like it should have an effect on the dataset that was worked with, since the text files, which measured the absolute magnetic field, were used. However, the former anomaly could possibly lead to many days having counts about the threshold without actual geomagnetic activity happening. This seems to be seen when comparing the day counts of SAM-III and GIMA in the H- and z-component plots. Most of the years in the H- and z-component plots have GIMA as having more counts than SAM-III which is expected, however, there are a few other years that also have SAM-III having more counts. In 2013, GIMA had gaps of data missing throughout the year which caused the low count and in 2011 and 2019 SAM-III had more counts but a closer look into the datasets is required to better understand why these occurred. Looking at the $\delta H/\delta t$ plots, GIMA seemed to have a fairly high count of measurements above both thresholds and further look into why this is, exactly, is also required. It was found that some of these counts were due to erroneous infinity values.

Erroneous Data

The data from 2010 to 2023 was not perfectly continuous and some of the calculations made during the creation of the dataset could've been done incorrectly. These would produce erroneous data consisting of Not-a-Number (NaN) and Infinity (Inf) values in the pandas DataFrame. After resampling both datasets into minute readings, roughly 1.5% (9935 rows) of SAM-III data contained NaN values and 0.00002% (110 rows) contained Inf values. With GIMA, 22% (1449380 rows) of the data contained NaN values and 0.014% (89443 rows) had Inf values. The NaN values seem to be the cause of missing data and the Inf values could possibly be from some of the calculations performed.

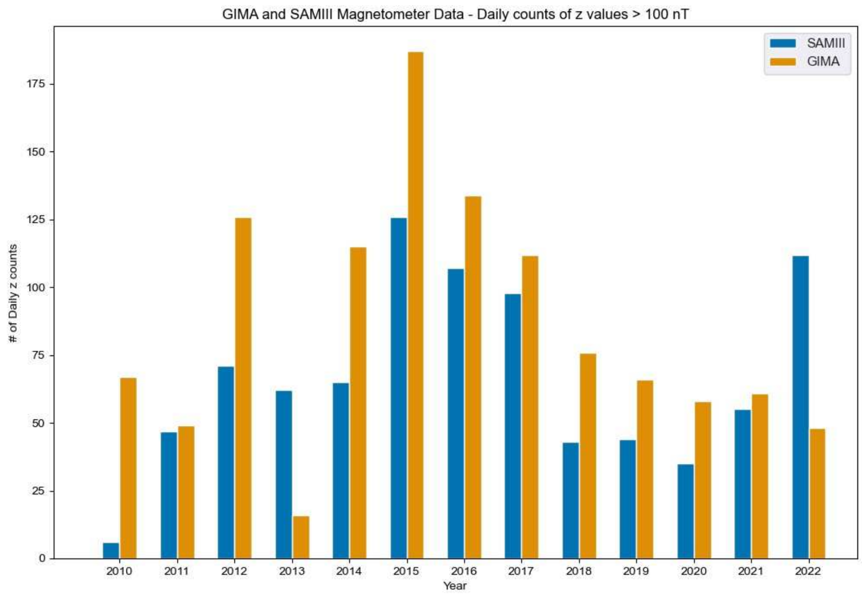

Figure 7: Number of days with |z| > 100 nT compared with the sunspot number

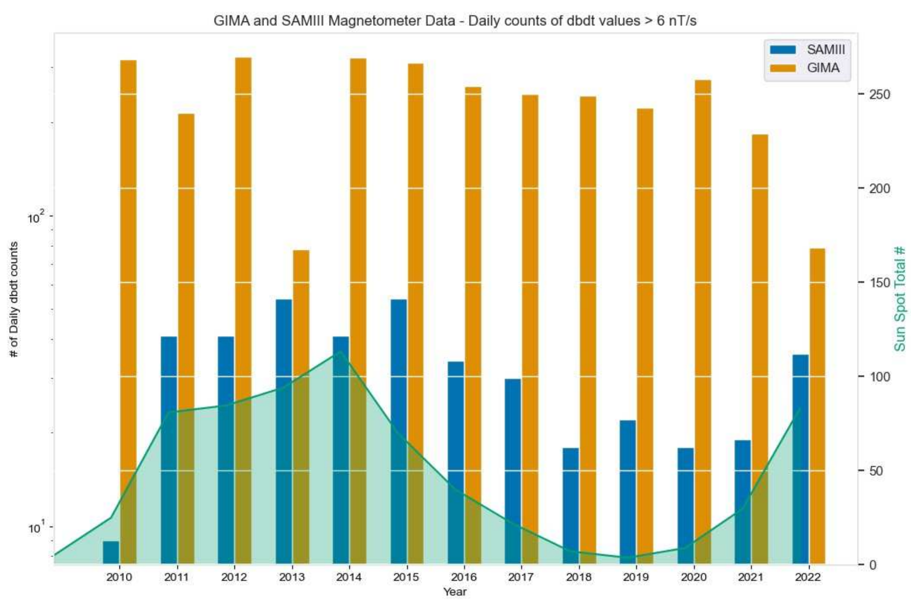

Figure 8: Number of days with |δH/δt| > 6 nT/s in log scale

Conclusion

As a semi-professional magnetometer, SAM-III seems to reliably measure geomagnetic disturbances as compared to GIMA's Trapper Creek magnetometer in each component in addition to solar activity as shown by the solar cycle dependence with the yearly mean sunspot number. Conclusions cannot be made on the temperature dependencies of SAMIII at the moment and further investigation is required but it is actively being investigated with newly deployed SAM-III devices including a temperature sensor. Based on the $\delta H/\delta t$ performance it is recommended that SAM-III devices be run with the highest temporal resolution possible with this already in action with current deployments of SAM-III taking measurements every 1 second instead of 10 seconds. The future will be promising to study the scientific and operational capabilities of SAM-III with higher temporal resolution in measurements and a temperature sensor in newer SWUG SAM-III deployments.

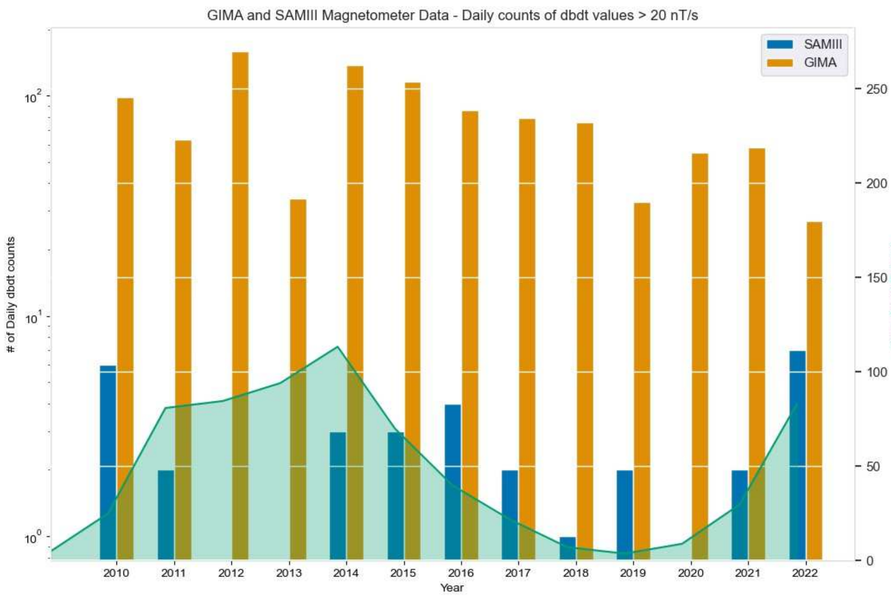

Figure 9: Number of days with |δH/δt| > 20 nT/s in log scale

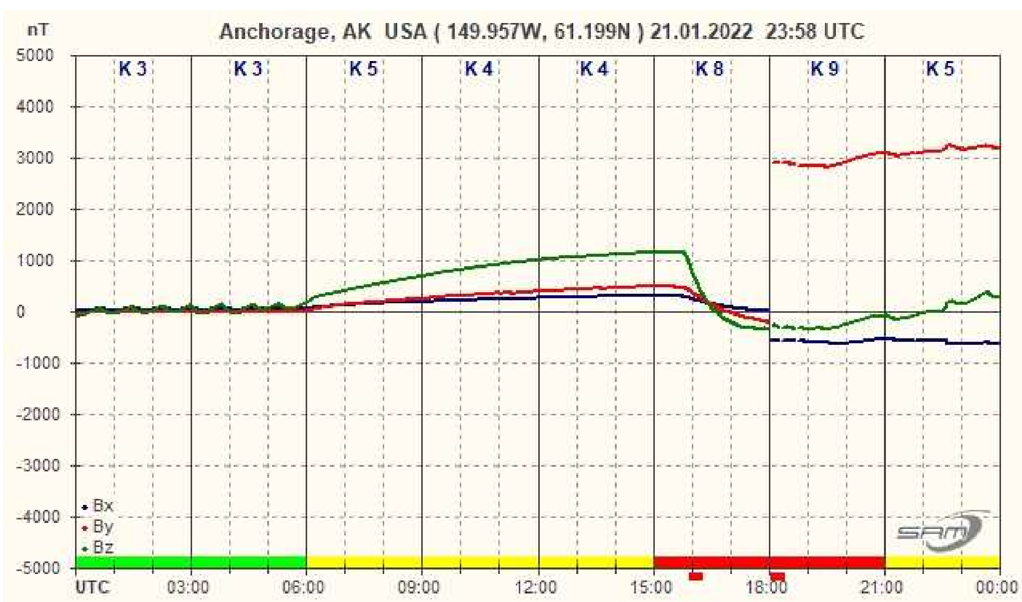

Figure 10: SAM-III - January 21st, 2022

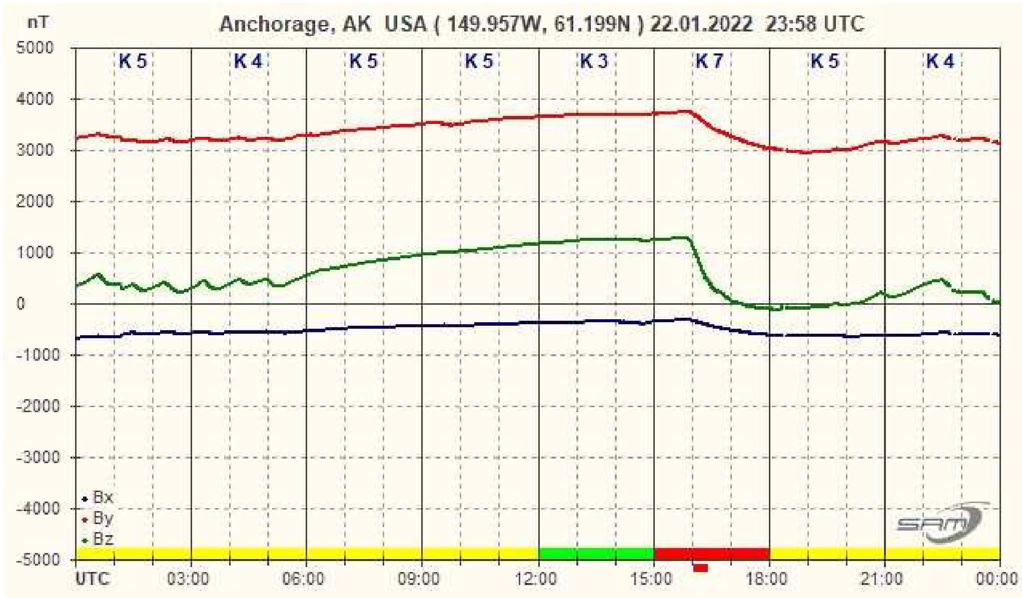

Figure 11: SAM-III - January 22nd, 2022

References

[1] A. Pulkkinen, E. Bernabeu, A. Thomson, A. Viljanen, R. Pirjola, D. Boteler, J. Eichner, P. J. Cilliers, D. Welling, N. P. Savani, R. S. Weigel, J. J. Love, C. Balch, C. M. Ngwira, G. Crowley, A. Schultz, R. Kataoka, B. Anderson, D. Fugate, J. J. Simpson, and M. MacAlester. Geomagnetically induced currents: Science, engineering, and applications readiness. *Space Weather*, 15(7):828–856, 2017.

[2] SAM Magnetometer Network. http://www.sam-magnetometer.net/index.html, 2023. Accessed on: 17 5 2023.

[3] Reeve Engineers. SAM3 Construction Manual. https://reeve.com/Documents/SAM/SAM3ConstructionManual.pdf, 2023. Accessed on: 17 5 2023.

[4] Reeve Engineers. Sam3 software setup. https://reeve.com/Documents/SAM/ SAM3SoftwareSetup.pdf, 2023. Accessed on: 10 5 2023.

[5] The pandas development team. pandas-dev/pandas: Pandas, February 2020.

[6] Hunter Barndt. Sam-iii parsing and data analysis tools. https://github.com/ whbarndt/samIII-magnetometer-data-analysis, 2023. Accessed on: 10 5 2023.

[7] R. Schunk and A. Nagy. *Ionospheres: Physics, Plasma Physics, and Chemistry*. Cambridge Atmospheric and Space Science Series. Cambridge University Press, 2009.

[8] B.B. Narod and J.R. Bennest. Ring-core fluxgate magnetometers for use as observatory variometers. *Physics of the Earth and Planetary Interiors*, 59(1):23–28, 1990.

[9] D. Wilkinson and Matt Heavner. Geophysical institute magnetometer array. *AGU Fall Meeting Abstracts*, 01 2006.

[10] Magnetometer Archive - Geophysical Institute, University of Alaska Fairbanks. https://www.gi.alaska.edu/monitors/magnetometer/archive, 2023. Accessed on: 17 5 2023.

[11] Magnetometer data, geophysical institute, uaf. Retrieved from Research Computing Systems 17 3 2023, 2010 - 2022.

[12] SIDC - Solar Influences Data Analysis Center: The sunspot index and long-term solar observations. https://www.sidc.be/silso/infosnytot, 2023. Accessed on: 28 3 2023.

[13] AK RWIS (Alaska road weather information system). https://mesonet.agron.iastate.edu/request/rwis/fe.phtml?network=AK_RWIS, 2023. Accessed on: 10 5 2023.

[14] S. E. Milan, S. M. Imber, A. L. Fleetham, and J. Gjerloev. Solar cycle and solar wind dependence of the occurrence of large dB/dt events at high latitudes. *Journal of Geophysical Research: Space Physics*, 128(4):e2022JA030953, 2023. e2022JA030953 2022JA030953.

[15] M. J. Engebretson, V. A. Pilipenko, L. Y. Ahmed, J. L. Posch, E. S. Steinmetz, M. B. Moldwin, M. G. Connors, J. M. Weygand, I. R. Mann, D. H. Boteler, C. T. Russell, and A. V. Vorobev. Nighttime magnetic perturbation events observed in Arctic Canada: 1. survey and statistical analysis. *Journal of Geophysical Research: Space Physics*, 124(9):7442–7458, 2019.